Available online at www.sciencedirect.com
SCIENCE DIRECT®
Journal of Colloid and Interface Science 261 (2003) 402–410
JOURNAL OF Colloid and Interface Science
www.elsevier.com/locate/jcis

Zeta-potential measurement using the Smoluchowski equation and the slope of the current–time relationship in electroosmotic flow

Alice Sze, David Erickson, Liqing Ren, and Dongqing Li *

Department of Mechanical and Industrial Engineering, University of Toronto, 5 King's College Road, Toronto, Ontario, Canada M5S 3G8

Received 26 November 2002; accepted 28 January 2003

Abstract

The ζ-potential of a solid–liquid interface is an important surface characterization quantity for applications ranging from the development of biomedical polymers to the design of microfluidic devices. This study presents a novel experimental technique to measure the ζ-potentials of flat surfaces. This method combines the Smoluchowski equation with the measured slope of current–time relationship in electroosmotic flow. This method is simple and accurate in comparison with the traditional streaming potential and electrophoresis techniques. Using this method the ζ-potentials of glass and poly(dimethylsiloxane) (PDMS) coated surfaces in KCl and $LaCl_3$ aqueous solutions were measured using several flow channels ranging from 200 to 300 μm in height. The ζ-potential was found to vary from −88 to −66 mV for glass surface and −110 to −68 mV for PDMS surfaces depending on the electrolyte and the ionic concentration. The measured values of the ζ-potential are found to be independent of the channel size and the applied driving voltage and generally are repeatable within ±6%.

Keywords: Electroosmosis; ζ-potential; Glass; PDMS

1. Introduction

When a solid surface is in contact with an aqueous solution, the formation of an interfacial charge causes a rearrangement of the local free ions in the solution to produce a thin region of nonzero net charge density near the interface. The arrangement of the charges at the solid–liquid interface and the balancing counterions in the liquid is usually referred to as the electrical double layer (EDL). There is a thin layer of counterions immediately next to the charged solid surface, called the compact layer. The counterions in the compact layer are immobile due to the strong electrostatic attraction. Counterions outside the compact layer are mobile. This part of the EDL is called the diffuse layer. The zeta (ζ) potential is the electrostatic potential at the boundary dividing the compact layer and the diffuse layer. The zeta potential is an important parameter for a number of applications including characterization of biomedical polymers [1,2], electrokinetic transport of particles [3,4] or blood cells [5], membrane efficiency [6,7], and microfluidics [8–10]. The understanding of the distinct colloidal and interfacial phenomena associated with these applications requires the knowledge of the ζ-potential.

The importance of the ζ-potential to so many applications in science and engineering has lead to the development of a number of techniques for measuring this quantity, based on one of the three electrokinetic effects: electrophoresis, electroosmosis, and the streaming potential [11]. In the electrophoresis method [11–13], the ζ-potential is determined by placing fine particles in an electric field and measuring their mobility, υ_E, using a suitable microscopic technique. The mobility is then related to the ζ-potential at the interface using the Smoluchowski equation [14],

$$\upsilon_E = 4\pi\varepsilon_0\varepsilon_r\frac{\zeta}{6\pi\mu}(1+\kappa r), \tag{1}$$

where ε_0 and ε_r are the relative dielectric constant and the electrical permittivity of a vacuum respectively, μ is the solution viscosity, r is the particle radius and $\kappa = (2n_0z^2e^2/\varepsilon_r\varepsilon_0k_BT)^{1/2}$ is the Debye–Hückel parameter, n_0 is the bulk ionic concentration, z is the valence of the ion, e is the charge of an electron, k_B is the Boltzmann constant, and T is the absolute temperature. This technique has been applied to characterize flat surfaces by initially grinding then into fine particles; for example, see Sanders et al. [15].

* Corresponding author.
E-mail address: dli@mie.utoronto.ca (D. Li).

0021-9797/03/$ – see front matter
doi:10.1016/S0021-9797(03)00142-5

However, it is unclear if the surface electrostatic properties of these particles are equivalent to the precrushed surfaces.

The streaming potential technique has been extensively applied to flat polymer and glass surfaces to study solid–liquid interface electrical properties [16–19] in a parallel plate microchannel. In this technique the downstream convection of ions via pressure driven flow induces a streaming potential which, for steady incompressible and laminar flow, can be related to the ζ-potential via

$$\frac{E_s}{\Delta P} = \frac{\varepsilon_r \varepsilon_0 \zeta}{\mu} \frac{1}{(\lambda_b + 2\lambda_s/h)}, \tag{2}$$

where E_s is the streaming potential, ΔP is the pressure difference, h is the channel height, λ_b is the bulk conductivity, and λ_s is the surface conductivity (a more detailed theoretical model of the streaming potential was described recently by Erickson et al. [20]). While this technique is inherently suitable for flat surfaces, accurately measuring the streaming potential may not be simple in practice. Additionally, both ζ and λ_s must be determined, which requires a series of measurements of E_s and ΔP at several different channel heights [20].

Most lab-on-a-chip devices use electroosmotic flow to transport solutions in microchannels. The electroosmotic flow in these applications may be uniquely influenced by such effects as joule heating or electrophoretically induced double-layer rearrangement (particularly important when heterogeneous surfaces are considered [21]) which may, in turn, influence the ζ-potential. Therefore, it is highly desirable to measure the ζ-potential under the electroosmotic flow condition. In this paper a new method is proposed for measuring the ζ-potential of flat solid surfaces by combining the Smoluchowski equation with the measured slope of current–time relationship in electroosmotic flow. It is obvious that the measurement of the total electrical current in electroosmotic flow is relatively simple and easy in comparison with the measurements in the electrophoresis and streaming potential methods. Because this approach uses electroosmotic flow, as opposed to pressure-driven flow in the streaming potential case, it is more representative of the true operating conditions of a microfluidic device. This approach also allows the use of flat surfaces, which are more flexible than capillary tubes in terms of surface treatment (for example microcontact printing) [22]. In the following sections the proposed technique and apparatus are described in detail. This technique is used to measure the ζ-potential of glass- and poly(dimethylsiloxane) (PDMS)-coated surfaces in several aqueous solutions.

2. Electroosmotic flow—current monitoring technique

The theory of electroosmosis was first set out in its present form by von Smoluchowski. When an electrical field is applied tangentially to a solid–liquid interface, an electrical body force is exerted on the excess counterions in the diffuse layer of the EDL. The ions will move under the influence of this applied electrical field, pulling the liquid with them and resulting in an electroosmotic flow. Consider an electroosmotic flow of an aqueous solution in a parallel-plate microchannel, as shown in Fig. 1. Generally most electroosmotic flows, owing to the inherently low Reynolds number, reach a steady state very quickly and the entrance length tends to be extremely short. For the case examined here the time to reach a steady state is on the order of 10 μm and the entrance length is approximately 10 μm. In addition the slit channel geometry, where the width is much larger than the height, $w \gg a$ (see Fig. 1), minimizes the edge effects and makes the velocity profile essentially uniform along the x-axis. As such the flow could be assumed as steady, one-dimensional, and fully developed. If κa is large (e.g., thin double layer or large channel height), it can be shown from the Smoluchowski equation that the average electroosmotic flow velocity is given by

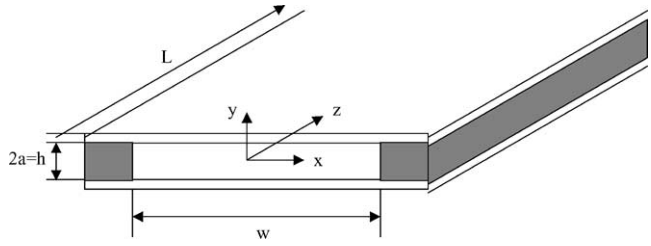

Fig. 1. Schematic of a parallel-plate microchannel.

$$v_{av} = \frac{\varepsilon_r \varepsilon_0 \zeta}{\mu} E_z, \tag{3}$$

where E_z is the applied electric field strength. The average velocity of an electroosmotic flow can be determined by monitoring the change in the electric current as one electrolyte solution replaces a slightly less concentrated one (or vice versa) in a capillary [22,23]. An experimental set-up used for such a measurement is shown in Fig. 2a. Briefly, reservoir 2 is filled with an electrolyte solution at a desired concentration while reservoir 1 and the capillary tube are filled with the electrolyte solution at a concentration of 95% of that in reservoir 2. After placing the ends of the capillary tube in reservoirs 1 and 2, a high-voltage electric field is applied to induce an electroosmotic flow through the capillary tube. During the electroosmosis, the higher concentration electrolyte solution from reservoir 2 migrates into the capillary tube, displacing an equal volume of lower concentration electrolyte solution. As a consequence, the total resistance of the liquid in the capillary tube changes and the current increases, as is shown in Fig. 2b [24]. Once the lower concentration solution in the tube is completely replaced by the higher concentration solution from reservoir 2, the current will reach a constant maximum value. The time for the current to reach the plateau value is the time required to complete the filling of the capillary tube via the electroosmotic

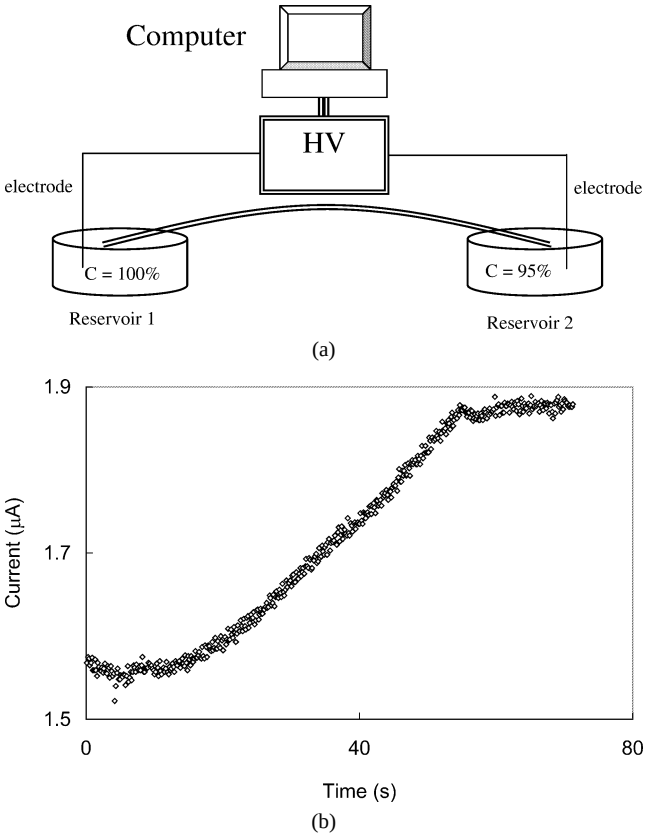

Fig. 2. (a) Schematic of the experimental setup used to measure the current variation and the complete displacement time for a two-concentration system during electroosmosis. (b) typical result of current vs time.

flow and thus can be related to the average velocity via

$$v_{\mathrm{av}} = \frac{L}{\Delta t}, \tag{4}$$

where, as before, L is the total length of the channel. v_{av} can then be related to the ζ-potential via Eq. (3).

The current monitoring technique offers a simple method for measuring the ζ-potential under conditions similar to those encountered in microfluidic transport applications. However, a major problem associated with this technique is the difficulty of determining the exact time required for one solution to completely displace the other, due to small current fluctuations and the gradual transitions at the beginning and end of the replacement process, as can be seen in Fig. 2b.

To avoid the above-mentioned problem, a new method was introduced [22] to evaluate the average electroosmotic velocity in a microchannel by using the slope of the current–time relationship. It was observed that, despite the curved beginning and ending sections, the measured current–time relationship is linear if the concentration difference is small. In other words, only the middle section of the current–time relationship is needed to calculate the constant slope. Thus a more accurate estimate of the average velocity could be obtained from the slope of this relationship. The slope of this current–time relationship is given by

$$\mathrm{slope} = \frac{\Delta I}{\Delta t}, \tag{5}$$

where ΔI and Δt are the changes in current and time over the linear range. In electroosmotic flow, the total current consists of three components: the bulk conductivity current, $I_{\mathrm{cond,\ bulk}}$, the surface conduction current, $I_{\mathrm{cond,\ surf}}$, and the convection current, I_{conv}. Generally, the convection current can be neglected when the total current is determined, since it is several orders of magnitude smaller than the other two current components. Then, under an applied electrical field, E_{z}, the total current can be shown as

$$I_{\mathrm{total}} = I_{\mathrm{cond,\ bulk}} + I_{\mathrm{cond,\ surf}} = \lambda_{\mathrm{b}} A_{\mathrm{cross}} E_{\mathrm{z}} + \lambda_{\mathrm{s}} L E_{\mathrm{z}}. \tag{6}$$

Substituting Eq. (6) for the difference of the current (Note: $\Delta\lambda_{\mathrm{s}} = 0$), Eq. (5) can be rewritten as

$$\begin{aligned}\mathrm{slope} &= \frac{\Delta(E_{\mathrm{z}} A_{\mathrm{cross}} \lambda_{\mathrm{b}})}{\Delta t} = \frac{\Delta(E_{\mathrm{z}} A_{\mathrm{cross}} \lambda_{\mathrm{b}})}{\Delta t}\frac{L}{L} \\ &= v_{\mathrm{av}} \frac{E_{\mathrm{z}} A_{\mathrm{cross}} (\lambda_{\mathrm{b2}} - \lambda_{\mathrm{b1}})}{L},\end{aligned} \tag{7}$$

where $(\lambda_{\mathrm{b2}} - \lambda_{\mathrm{b1}})$ is the difference in bulk conductivity between the high-concentration solution and the low concentration solution. Rearranging Eq. (7) yields

$$v_{\mathrm{av}} = \frac{\mathrm{slope} \cdot L}{E_{\mathrm{z}} A_{\mathrm{cross}} (\lambda_{\mathrm{b2}} - \lambda_{\mathrm{b1}})}. \tag{8}$$

The above expression shows that the average electroosmotic flow velocity can be determined by measuring the slope of the current–time relationship. By using the slope of the current–time relationship, the difficulty in determining the exact beginning and end of the displacement process in the current monitoring method can be avoided. Once the average velocity is determined, one can use the v_{av} value and Eq. (3) to determine the ζ-potential. In other words, combining Eq. (8) and Eq. (3) gives

$$\zeta = \frac{\mu \cdot \mathrm{slope} \cdot L}{\varepsilon_{\mathrm{r}} \varepsilon_0 E_{\mathrm{z}}^2 A_{\mathrm{cross}} (\lambda_{\mathrm{b2}} - \lambda_{\mathrm{b1}})}. \tag{9}$$

In the following section, an experimental set-up to measure the slope of the current–time relationship in the electroosmotic flow to determine the ζ-potentials of flat solid surfaces will be described.

3. Methods and materials

3.1. Experimental apparatus

The new experimental apparatus consists of three major parts: a microchannel cell (Fig. 3a), a liquid handling system (Fig. 3b), and an electroosmotic flow monitoring system (Fig. 3c). The microchannel cell itself consists primarily of a parallel-plate microchannel confined between an inlet reservoir block and an outlet reservoir block. The parallel-plate microchannel is formed by two flat sample surfaces

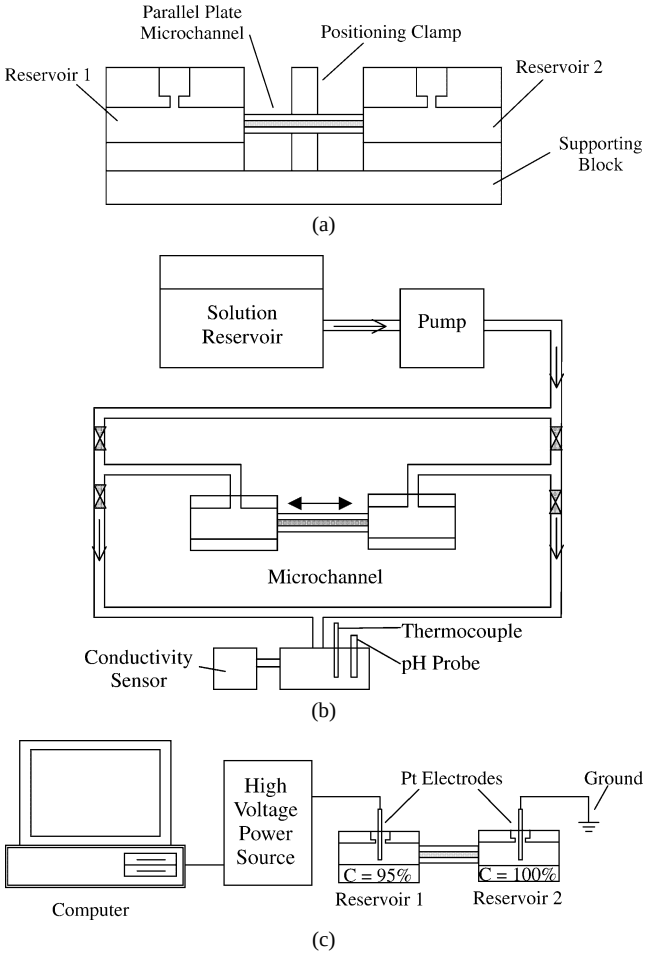

Fig. 3. Schematics of (a) the microchannel cell (cross-section), (b) the experimental setup used for liquid handing, and (c) the electroosmotic flow measuring system.

(15.5 × 37 mm). A positioning clamp is placed to keep the surfaces parallel and to limit their deflection when exposed to pressure (during the flushing step, explained in Section 3.4). The two equal-sized reservoirs form the inlet and the outlet to the microchannel.

The parallel-plate microchannels were made using two identical test surfaces separated by two thin plastic shims (Small Parts, Inc., Florida), which formed the channel sidewalls. The shims were placed along the lateral edges of the cleaned surfaces and fixed by applying a small amount of epoxy (Devcon, USA), leaving a flow passage 3.5 mm wide. Once formed the channel was allowed to dry at room temperature air for 16 h. After that, the width and the length of the microchannel were measured using a precision gauge (Model CD-6″B, Mitutoyo Co., Japan) with an accuracy of ±1 μm. Finally, the microchannel was mounted in the supporting blocks, as illustrated in Fig. 3a, to form the microchannel cell. A positioning clamp was then used to maintain the channel position.

As it is the most sensitive dimension in terms of introducing systematic error into the experimental results, the channel height was measured by two independent techniques, direct digital imaging analysis and volume flow rate calibration. Using a microscope and video camera system (Model 4815-5000, Cohu; Wild Heerbrugg M7-5, Switzerland) with a 40× objective the channel height and parallel could be measured to an accuracy of ±0.8 μm prior to being placed in the experimental system. The channel heights used in this study range from 200 to 300 μm. The height measurements at the channel inlet and outlet was found to be consistent within ±2%. Once placed in the experimental system the channel height was also calibrated by using pressure driven flow of a highly concentrated electrolyte solution (e.g., 10^{-2} M) to minimize any electrical double layer effects. For a steady fully developed laminar flow, the channel height h can be related the measured pressure drop, ΔP, and volume flow rate, Q, via

$$\Delta P = \frac{Q}{h^3}\frac{12\mu L}{w}. \tag{10}$$

The pressure drop was measured using a differential pressure transducer (Validyne, Model CD23, Engineering Co., CA, USA) and volume flow rate through mass accumulation at the channel exit by using an electronic balance (Mettler Instrument AG, Model BB240) with an accuracy of 1 mg. The accuracy of the flow rate measurement was estimated to be ±2%. The discrepancy between the results of the channel height from the above two measuring methods was found to be within 2%, suggesting that an accurate estimate of the true channel height had been obtained.

A liquid handling system has been designed (Fig. 3b) to clean the system after each run and introduce new solutions. Prior to the experiment, pure water is pumped from a solution reservoir to the flow loop and though the microchannel for at least half an hour by a high-precision pump (Masterflex, Model 7550-60, Barnant Co., IL), which has a flow rate range of 0.6 to 2900 ml/min. Then the flushing process was repeated using the test solution until the electrical conductivity of the test solution exiting the microchannel reaches and remains at the standard value for the specific electrolyte solution at the given concentration. The bulk electrical conductivity is measured using a conductivity sensor (Model Inpro 7001/120, Mettler Toledo Process Analytical Inc., MA), which is connected to a conductivity/resistivity transmitter (CR7300, Mettler Toledo Process Analytical Inc., MA).

The electroosmotic flow monitoring system, shown in Fig. 3c, consists primarily of the measuring cell with electrodes, a high-voltage power source (CZE 1000R, Spellman High Voltage Electronics Co., NY), and a PGA-DAS 08 data acquisition card (OMEGA Engineering, Quebec, Canada). During the experiments, the high-voltage power source was used to apply a potential difference between the two reservoirs via platinum electrodes. The output voltage and current were recorded on a personal computer, via the data acquisition card, using an output signal at 0–10 V from the power supply.

3.2. Surface preparation

Glass surfaces were prepared from microscope slides, which had been cut and carefully polished to a dimension of 15.5 by 37 mm, with an accuracy of ±0.5 mm. The glass plates were soaked in acetone (Caledon Laboratories Ltd., ON, Canada) for 12 h and then vigorously washed with acetone several times. After that, the surfaces were submerged in deionized ultrafiltered water (DIUF) (Fisher Scientific, Canada) for 12 h. The surfaces were then dried under a heat lamp before use.

Many microfluidic devices reported in the literature have been fabricated in glass; for example, see Woolley et al. [25]. Recently, however, polymeric material has been explored as an alternative for the fabrication of microfluidic systems, in particular poly(dimethylsiloxane) (PDMS) [26, 27]. PDMS is a bulk polymer consisting of repeated units of $–OSi(CH_3)_2O–$ and was first introduced for microfluidic devices by Kumar and Whitesides [28] in 1993. Since then it has become a popular material for building microfluidic devices for a number of reasons: (i) it is much less expensive than glass and not as fragile as glass; (ii) channels can be formed by molding or embossing rather than etching; (iii) it is optically transparent down to 280 nm, so it can be used for a number of detection schemes; (iv) it cures at low temperatures; (v) it can be sealed reversibly to itself and a range of other materials, such as glass, by making molecules contact with the surface; and (vi) it is nontoxic—mammalian cells can be cultured directly on it [29,30].

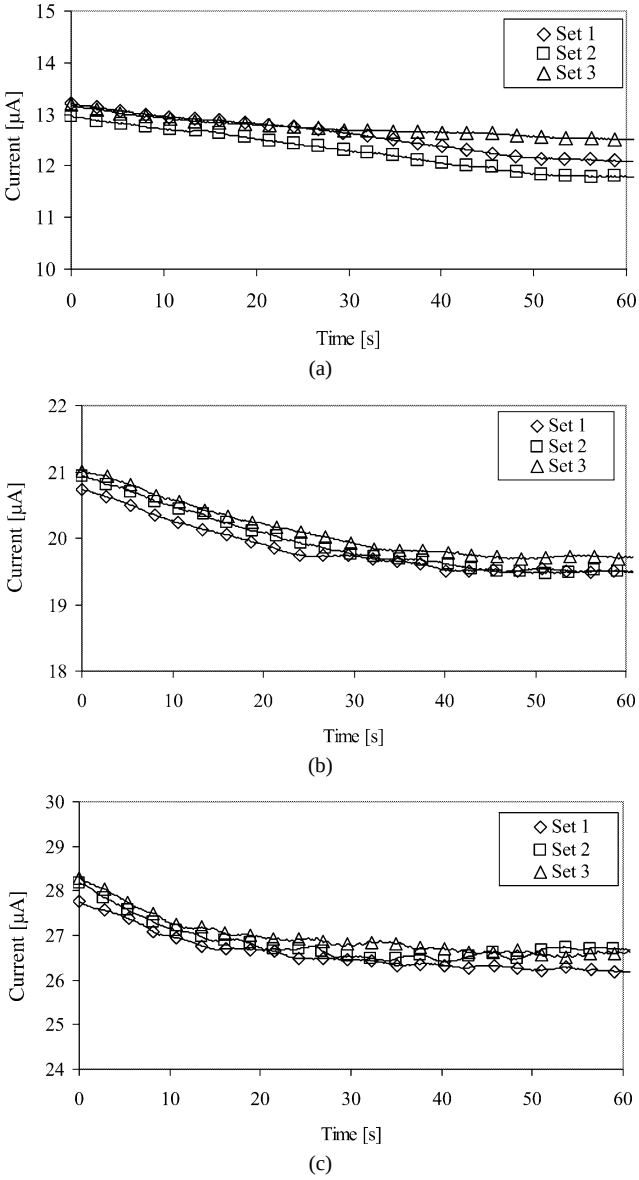

Fig. 4. Current vs time for 10^{-4} M KCl solution in a glass channel of 217 μm under an applied voltage of (a) 400 V, (b) 600 V, and (c) 800 V over the 37-mm length of the channel.

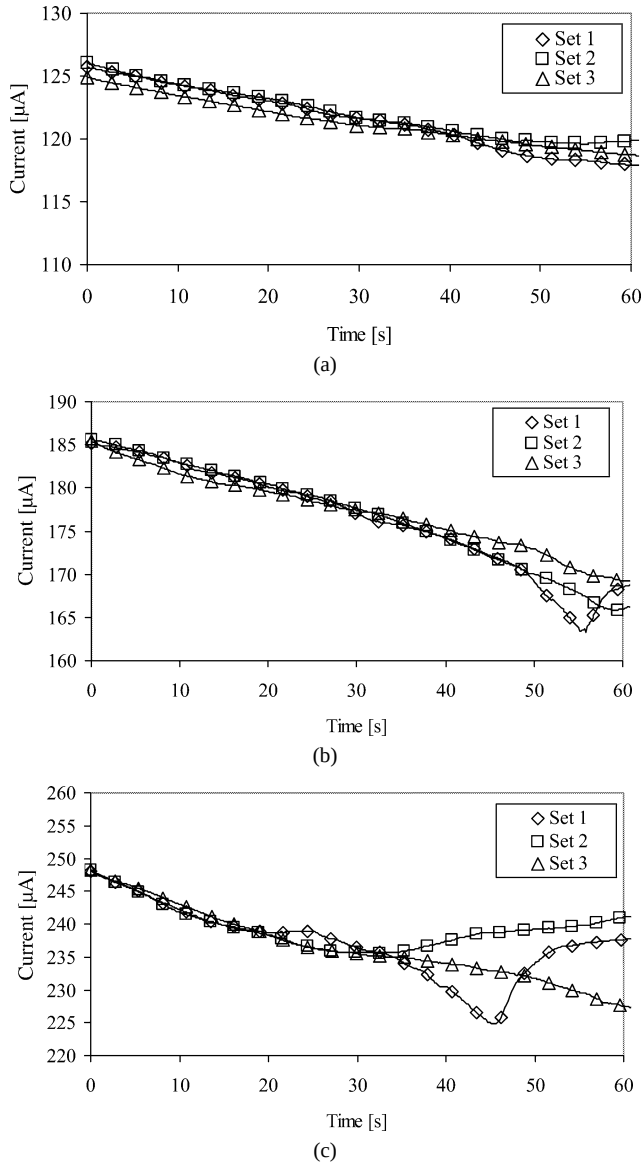

Fig. 5. Current vs time for 10^{-3} M KCl solution in a glass channel of 217 μm under an applied voltage of (a) 400 V, (b) 600 V, and (c) 800 V over the 37-mm length of the channel.

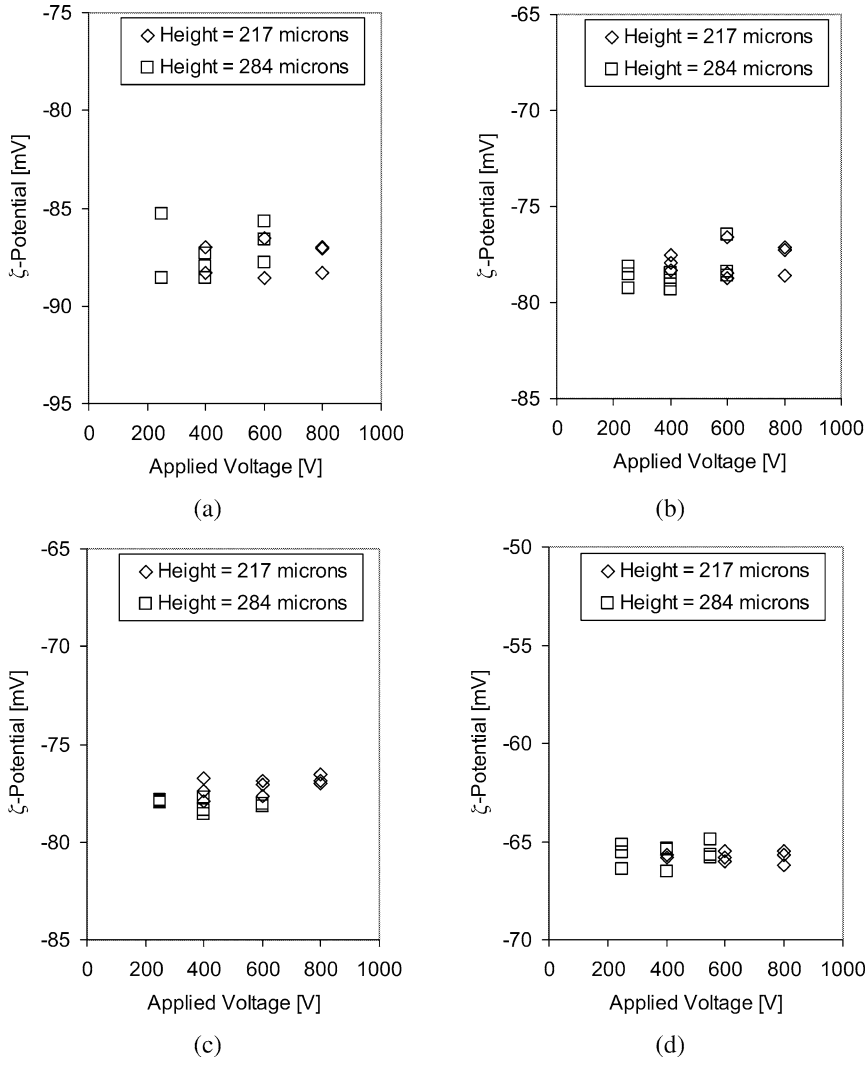

Fig. 6. ζ-potential vs applied voltage and channel height for glass surfaces in (a) 10^{-4} M KCl, (b) 10^{-3} M KCl, (c) 10^{-4} M $LaCl_3$, and (d) 10^{-3} M $LaCl_3$ aqueous solutions.

For the PDMS-coated glass surfaces, each glass plate was fixed to a glass dish lined with parchment paper. PDMS base and curing agent (Sylgard 184, Dow Corning, Midland, MI, USA) were thoroughly mixed in a ratio of 10:1 and then poured onto the cleaned surfaces. The PDMS was then degassed at room temperature for 1 h to permit the removal of air bubbles. The glass dishes were then put in an oven at 65 °C for 30 min. After cooling, the PDMS-coated glass surfaces were removed from the dishes and cleaned with acetone and DIUF water.

3.3. Solution preparation

Aqueous KCl and aqueous $LaCl_3$ solutions were chosen for these experiments for two reasons. First, the electrokinetic characteristics of these solutions in contact with various solid surfaces have been well studied by several researchers using a variety of other techniques [14,31], allowing a direct comparison with the results obtained here. Second, the effect of the valence and the symmetry of the ions on the flow characteristics in a microchannel could be examined, since the KCl solution has symmetrical 1:1 ions (the valence is 1), while the $LaCl_3$ has an unsymmetrical ion distribution, and the valence of the La^+ ion is 3.

The electrolyte solutions were prepared by dissolving KCl (Bioshop Canada Inc., ON, Canada) or $LaCl_3{\cdot}H_2O$ (Fisher Scientific Co., NJ, USA) in DIUF water, which has pH 6.5 and $\lambda_b = 1.16\ \mu S\,cm^{-1}$ at 25 °C. The bulk liquid conductivities of the solutions were measured using a high-precision conductivity meter with an accuracy of ±0.5% of its reading. The measured conductivities of the aqueous solutions used here were 10^{-4}M KCl with $\lambda_b = 16.3\ \mu S\,cm^{-1}$, 10^{-3} M KCl with $\lambda_b = 146.0\ \mu S\,cm^{-1}$, 10^{-4} M $LaCl_3$ with $\lambda_b = 41.1\ \mu S\,cm^{-1}$, and 10^{-3} M $LaCl_3$ with $\lambda_b = 410.8\ \mu S\,cm^{-1}$.

3.4. Experimental procedure

Prior to the introduction of a test solution into the apparatus the microchannel cell and the entire piping system were bidirectionally rinsed with DIUF water for 1 h in order to remove any contaminants (such as electrolytes remaining from previous experiments). Following that, a second 15-min rinsing cycle was initiated using the desired test solution. The transparent nature of the microchannel surfaces allowed visual inspection of the channel to ensure that all bubbles had been removed. Once the flushing was complete, the microchannel cell was detached from the liquid-handling system and the temperature, pH level, and bulk conductivity of the solution in the reservoirs were measured, while any fluid height difference between the two reservoirs was allowed to equilibrate. The content of reservoir 1 was then diluted to 95% of the test solution by pipetting a predetermined amount of DIUF water (an equivalent volume was also removed from the reservoir to ensure the system remained at mechanical equilibrium).

Once both reservoirs and the microchannel were filled with electrolyte, the electroosmotic flow measurement began. Immediately after placing the platinum electrodes into each reservoir and ensuring that they were aligned perpendicular to the channel, a voltage difference was applied. The lower concentrated electrolyte from reservoir 1 thus gradually displaced the higher concentrated electrolyte in the microchannel, increasing the overall channel resistance and thus decreasing the current draw, which was monitored via the data acquisition system. The voltage was applied for no longer than 1 min, after which the power supply was switched off and the electrodes were removed from the microchannel cell. All experiments were repeated in triplicate and conducted at room temperature, 25 °C.

4. Results and discussion

As mentioned earlier, the purpose of this study was to measure the ζ-potential of glass and PDMS surfaces using the system described above. Measurements were made using four different channel heights (217, 229, 284, and 298 μm) and four different solutions (10^{-3} M and 10^{-4} M KCl and $LaCl_3$, respectively) over a range of applied voltages from 100 to 800 V (applied over the 37-mm length of the channel).

4.1. Glass surfaces

As examples, Figs. 4 and 5 show the current change with time for 10^{-4} M and 10^{-3} M KCl solutions with glass surfaces at three different applied voltages. In all cases measurements were done three times to confirm the repeatability. As seen from these figures, a linearly decreasing relationship between current and time is evident for the first 20 s of each set. In the low-applied-voltage cases the current ultimately reaches a constant value when the high-concentration solution in the microchannel has been completely replaced by the lower concentration solution, such as Fig. 4a. In the high-concentration solution and high-electrical-field-strength cases, such as Fig. 5c, the current draw became unstable at the end of the experiment. It is believed that the fluctuation of the current value is due to the joule-heating effect. For these experiments, then, the slope current vs time was taken over the first 20 s of the displacement process in order to avoid this complication.

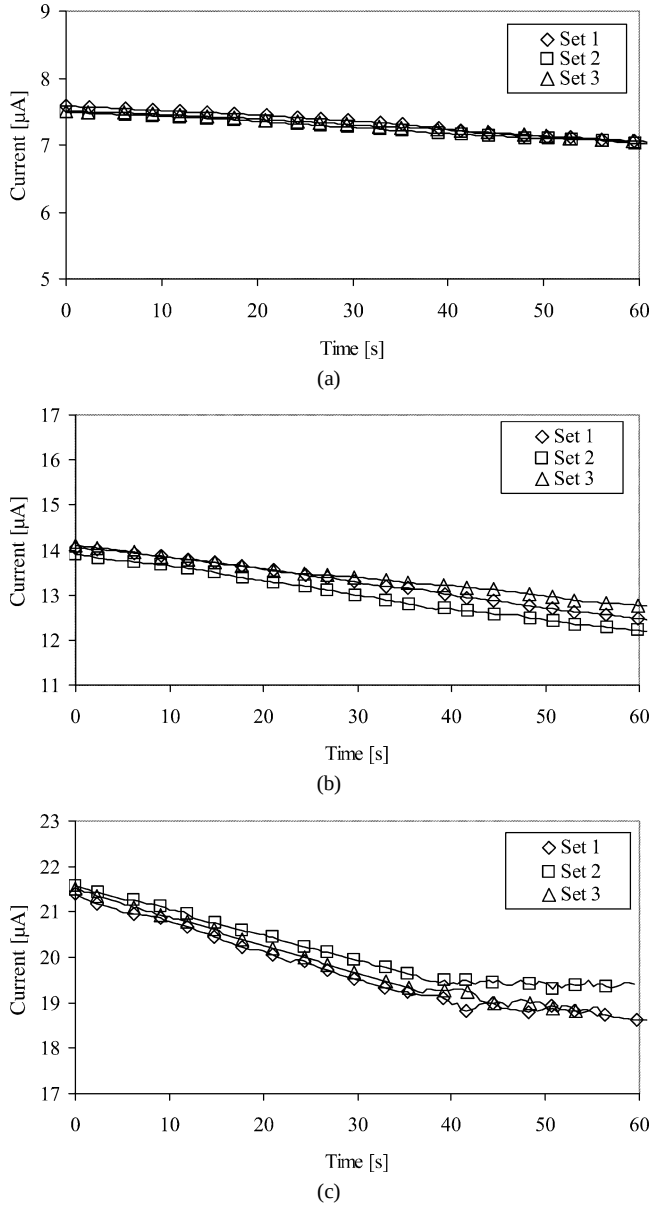

Fig. 7. Current vs time for a 10^{-4} M KCl solution in a PDMS-coated glass channel of 229 μm under an applied voltage of (a) 200 V, (b) 400 V, and (c) 600 V over the 37-mm length of the channel.

The slopes of the current–time relationship shown in the previous figures were used to determine the ζ-potential of the glass plate surface using Eq. (9) and the following physical properties of DIUF water: $\varepsilon_r = 80$, $\varepsilon_0 = 8.854 \times$

10^{-12} $CV^{-1}\,m^{-1}$, and $\mu = 0.001$ $N\,s\,m^{-2}$ [32]. Figure 6 shows calculated ζ-potential as a function of applied voltage and channel height for (a) 10^{-4} M KCl, (b) 10^{-3} M KCl, (c) 10^{-4} M $LaCl_3$, and (d) 10^{-3} M $LaCl_3$ solutions. As expected, the ζ-potential shows no dependence on the channel height or the magnitude of the applied field and the results were found to be repeatable within ±5%. From these results the ζ-potential was found to be −88 mV for 10^{-4} M KCl, −78 mV for 10^{-3} M KCl, −77 mV for 10^{-4} M $LaCl_3$, and −66 mV for 10^{-3} M $LaCl_3$. These values are similar to those obtained for glass surfaces using the electrophoresis technique [15] and the streaming potential technique [33].

4.2. PDMS-coated glass surface

For the PDMS-coated surfaces, a sample experimental result of current vs time for the 10^{-4} M solution in a microchannel with height of 229 μm is plotted in Fig. 7. As before, measurements under the same conditions were repeated three times to confirm the reproducibility, which was found to be within ±3%. For the PDMS coated surfaces the input voltage was reduced to a maximum of 600 V and thus the current fluctuation could be eliminated in most cases. As before, the slopes of the current–time relationship were measured over the initial 20-s time period.

Figure 8 shows the ζ-potential calculated by Eq. (9) against the applied voltage for (a) 10^{-4} M KCl, (b) 10^{-3} M KCl, (c) 10^{-4} M $LaCl_3$, and (d) 10^{-3} M $LaCl_3$ solutions. As in the previous cases of the glass surface, the ζ-potential shows no dependence on the channel height or the magnitude of the applied field and the measured results are reproducible within ±6%. Using these results the measured ζ-potential values were −110, −87, −82, and −68 mV for 10^{-4} M KCl, 10^{-3} M KCl, 10^{-4} M $LaCl_3$, and 10^{-3} M $LaCl_3$ solutions, respectively. Examination of Figs. 6 and 8 indicates that the magnitude of the ζ-potential for a PDMS-coated glass surface is higher than that for a glass surface under the same conditions. This is in agreement with the

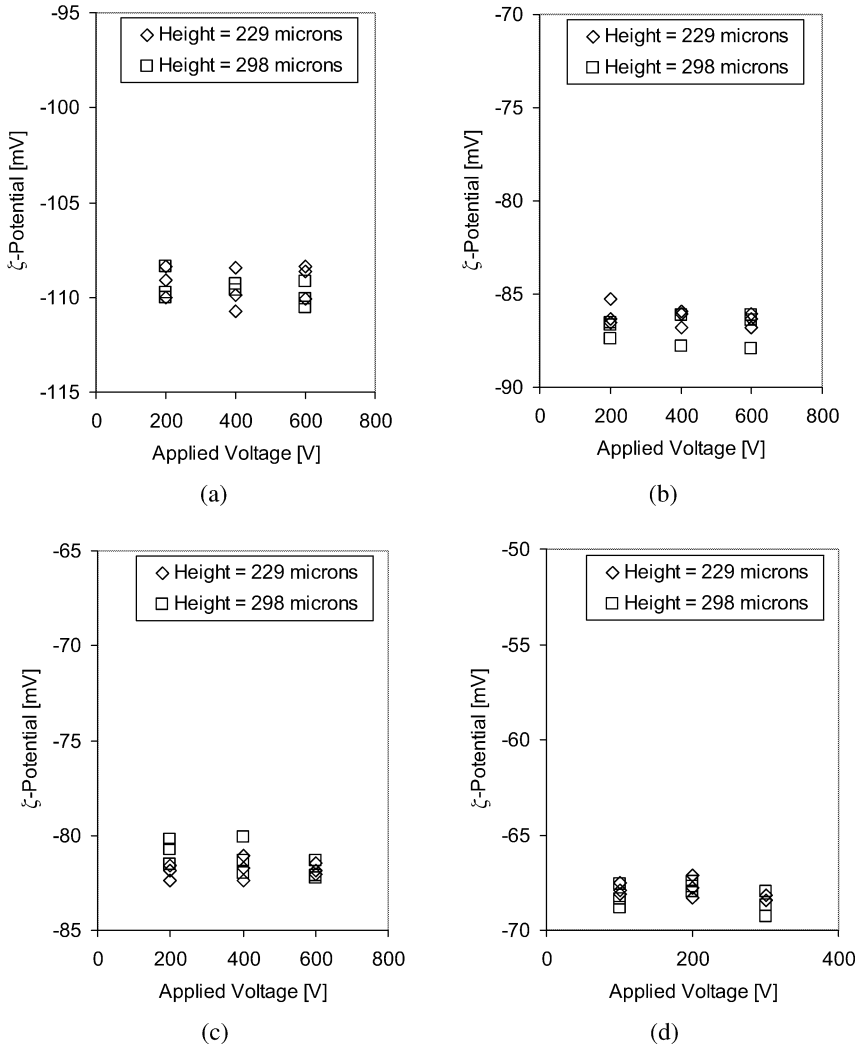

Fig. 8. ζ-potential vs applied voltage and channel height for PDMS surfaces in (a) 10^{-4} M KCl, (b) 10^{-3} M KCl, (c) 10^{-4} M $LaCl_3$, and (d) 10^{-3} M $LaCl_3$ aqueous solutions.

findings of other authors [16,17] for similar polymer surfaces.

5. Summary

The ζ-potential is an important parameter in the characterization of solid–liquid interfaces for a number of applications. The purpose of this research is to determine the ζ-potential of glass and PDMS-coated surfaces in contact with 10^{-4} M and 10^{-3} M aqueous KCl solutions and 10^{-4} M and 10^{-3} M aqueous $LaCl_3$ solutions by a technique combining the Smoluchowski equation with the measured slope of the current–time relationship in electroosmotic flow.

Using the new experimental method the ζ-potential was found to vary from -88 to -66 mV for glass and -110 to -68 mV for PDMS surfaces, depending on the electrolyte and the ionic concentration. These values were found to be independent of channel height and the magnitude of the applied electric field and were repeatable within $\pm 6\%$. The measurements involving a high electrolyte concentration and high applied voltage were limited due to joule-heating effects near the end of the experiment. By measuring the slope over the first 20 s of the experiment, however, the influence of this effect on the measured ζ-potential was minimized.

Acknowledgments

The authors to thank the Natural Sciences and Engineering Research Fund for financial support in the form of a scholarship to D. Erickson, a research grant to D. Li, and an Ontario Graduate Scholarship to L. Ren.

References

[1] C. Werner, U. König, A. Augsburg, C. Arnhold, H. Körber, R. Zimmermann, H.J. Jacobash, Colloids Surf. A 159 (1999) 519.
[2] C. Werner, H.J. Jacobash, Int. J. Artificial Organs 22 (1999) 160.
[3] C. Ye, D. Sinton, D. Erickson, D. Li, Langmuir, in press.
[4] H.J. Keh, J.L. Anderson, J. Fluid Mech. 153 (1985) 417.
[5] A.R. Minerick, A.E. Ostafin, H.C. Chang, Electrophoresis 23 (2002) 2165.
[6] J. Huang, X.L. Wang, W.S. Qi, X.H. Yu, Desalination 146 (2002) 345.
[7] Y. Shim, H.J. Lee, S. Lee, S.H. Moon, Cho, Env. Sci. Technol. 36 (2002) 3864.
[8] D. Erickson, D. Li, Langmuir 18 (2002) 1883.
[9] D. Ross, T. Johnson, L.E. Locascio, Anal. Chem. 73 (2001) 2509.
[10] N.A. Patankar, H.H. Hu, Anal. Chem. 70 (1998) 1870.
[11] D.F. Evans, H. Wennerström, The Colloidal Domain: Where Physics, Chemistry, Biology, and Technology Meet, Wiley–VCH, New York, 1999.
[12] H.A. Abramson, L.S. Moyer, H.M. Garin, Electrophoresis of Proteins, Reinhold, New York, 1942.
[13] H.J. Jacobasch, Acta Polym. 31 (1980) 481.
[14] R.J. Hunter, Zeta Potential in Colloid Science, Academic Press, New York, 1981.
[15] R.S. Sanders, R.S. Chow, J.H. Masliyah, J. Colloid Interface Sci. 174 (1995) 230.
[16] A. Voigt, H. Wolf, S. Lauckner, G. Neumann, R. Becker, L. Richter, Biomaterials 4 (1983) 299.
[17] C. Werner, H. Körber, R. Zimmermann, S. Dukhin, H.J. Jacobasch, J. Colloid Interface Sci. 208 (1998) 329.
[18] J. Jachowicz, M.D. Berthiaume, J. Colloid Interface Sci. 133 (1989) 118.
[19] R. Zimmermann, S. Dukhin, C. Werner, J. Phys. Chem. B 105 (2001) 8544.
[20] D. Erickson, D. Li, C. Werner, J. Colloid Interface Sci. 232 (2000) 186.
[21] D. Erickson, D. Li, submitted for publication.
[22] L. Ren, C. Escobedo-Canseco, D. Li, J. Colloid Interface Sci. 250 (2002) 238.
[23] X. Huang, M.J. Gordon, R.N. Zare, Anal. Chem. 60 (1988) 1837.
[24] S. Arulanandam, D. Li, J. Colloid Interface Sci. 225 (2000) 421.
[25] A.T. Woolley, K. Tao, A.N. Glazer, R.A. Mathies, Anal. Chem. 70 (1998) 684.
[26] C.S. Effenhauser, G.J.M. Bruin, A. Paulus, M. Ehrat, Anal. Chem. 69 (1997) 3451.
[27] R.S. Martin, A.J. Gawron, S.M. Lunte, C.S. Henry, Anal. Chem. 72 (2000) 3196.
[28] A. Kumar, G.M. Whitesides, App. Phys. Lett. 63 (1993) 2002.
[29] J.C. McDonald, D.C. Duffy, J.R. Anderson, D.T. Chiu, H. Wu, O.J.A. Schueller, G.M. Whitesides, Electrophoresis 21 (2000) 27.
[30] X. Ren, M. Bachman, C. Sims, G.P. Li, N. Albritton, J. Chromatography B 762 (2001) 117.
[31] L. Ren, D. Li, W. Qu, J. Colloid Interface Sci. 233 (2001) 12.
[32] R. Weast, M.J. Astle, W.H. Beyer, CRC Handbook of Chemistry and Physics, CRC Press, Boca Raton, FL, 1986.
[33] Y.G. Gu, D.Q. Li, J. Colloid Interface Sci. 226 (2000) 328.